

# Lactic acid–magnesium oxide nanocrystal interactions: how nanoparticle size and shape affect chemistry and template oligomerization

Erin M. Beavers,<sup>a</sup> Kenneth J. Klabunde,<sup>\*a</sup> Biobing Wang<sup>b</sup> and Susan Sun<sup>b</sup>

Received (in Montpellier, France) 23rd April 2009, Accepted 12th June 2009

First published as an Advance Article on the web 15th July 2009

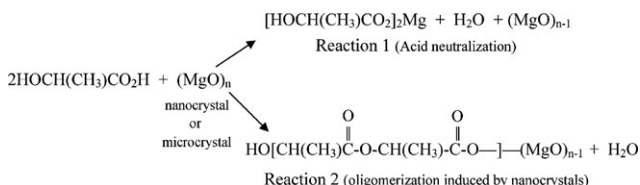
DOI: 10.1039/b908132a

L-Lactic acid was allowed to react with small amounts of commercial MgO, Nanoactive<sup>®</sup>, and Nanoactive Magnesium Oxide Plus<sup>®</sup> particles, each of which differs in surface area, shape, and reactivity. The reactions were carried out by refluxing the nanoparticles in a solvent suspension of methanol or propanol. Upon addition of the lactic acid monomer, at reflux temperature, two reactions competed with each other: (1) acid–base to yield magnesium lactate salt, and (2) oligomerization to yield a nanocomposite prepolymer. The products were characterized for thermal, chemical, and morphological properties. Additionally, titrations were performed to determine how much MgO was consumed by the acid, and how this changed with nanoparticle size and shape. Polymerization appears to initiate on the surface of the magnesium oxide particles, the results of which are physically unique composites of lactic acid and magnesium oxide, and final properties depend on MgO nanoparticle characteristics. One of the most interesting results was the finding that larger, less reactive MgO favored the acid–base neutralization reaction, while smaller, more reactive MgO particles favored the MgO induced oligomerization pathway.

## 1. Introduction

The chemistry of nanocrystalline materials can change depending on size and/or shape. Such differences are due to increased specific surface area coupled with enhanced surface reactivities due to a higher population of reactive corners, edges, and defects.<sup>1–6</sup>

A particularly interesting study would be to choose a system where competing reactions could take place, and determine if the nanocrystalline size/shape could influence reaction pathways, much in the same way that selectivities have often been used to learn about catalytic particle size/shape effects.<sup>7–12</sup> Herein, we report such a study: the interaction of L-lactic acid with magnesium oxide (MgO) nanocrystals. Different MgO nanocrystalline morphologies were employed (Fig. 1), and the competing reactions were (1) acid–base neutralization to form magnesium lactate (reaction 1), and nanocrystal aided oligomerization with loss of water (reaction 2, numerous chains could form on one nanocrystal):



Moreover, there is another reason for our interest in this system, and it involves the prospect of creating new and better

environmentally acceptable biopolymers—bio-nanocomposites. It is well known that inorganic fillers, such as nanoclays, can enhance thermal and impact stabilities substantially in classic polymers, such as polyethylene.<sup>13–17</sup> However, there has been little work where reactive nanoparticle<sup>2</sup> fillers have been studied, and essentially nothing has been reported regarding the combination of reactive nanoparticles and biopolymers, such as polylactic acid. Indeed, our first report in this area has noted that adding reactive nano-magnesium oxide to *preformed polylactic acid* does have significant positive effects on thermal properties.<sup>18</sup> Thus, we were interested in determining how reactive MgO nanocrystals interact with the monomer, lactic acid, and this has led to the results reported herein. Therefore, motivations for the work reported herein are (1) to determine if nanoparticle size/shape/surface area causes differences, and (2) to determine if monomer polymerization initially induced by nanoparticles yields differences vs. adding nanoparticles to preformed polymer.

Many nanoparticles are currently available commercially, including metal oxide powders of titania (TiO<sub>2</sub>), silica (SiO<sub>2</sub>), magnesium oxide (MgO), and alumina (Al<sub>2</sub>O<sub>3</sub>), to name a few. Additionally, silver and gold nanoparticles, as well as several semiconductor particles, can also be synthesized in the lab using various well-known techniques.<sup>19–21</sup> Perhaps the most widely-known class of nanomaterial used in the polymer industry, however, is the nanoclays, which includes hydro-talcite, octasilicate, mica fluoride, and the most common, montmorillonite.

Magnesium oxide nanoparticles, as well as many of their potential applications, have been well characterized.<sup>2</sup> There are three different forms of magnesium oxide that were used as additives in this study: commercial magnesium oxide (CM-MgO), Nanoactive<sup>®</sup> magnesium oxide (NA-MgO), and

<sup>a</sup> Department of Chemistry, Kansas State University, Manhattan, KS 66506, USA. E-mail: Kenjk@ksu.edu

<sup>b</sup> Department of Grain Science, Kansas State University, Manhattan, KS 66506, USA

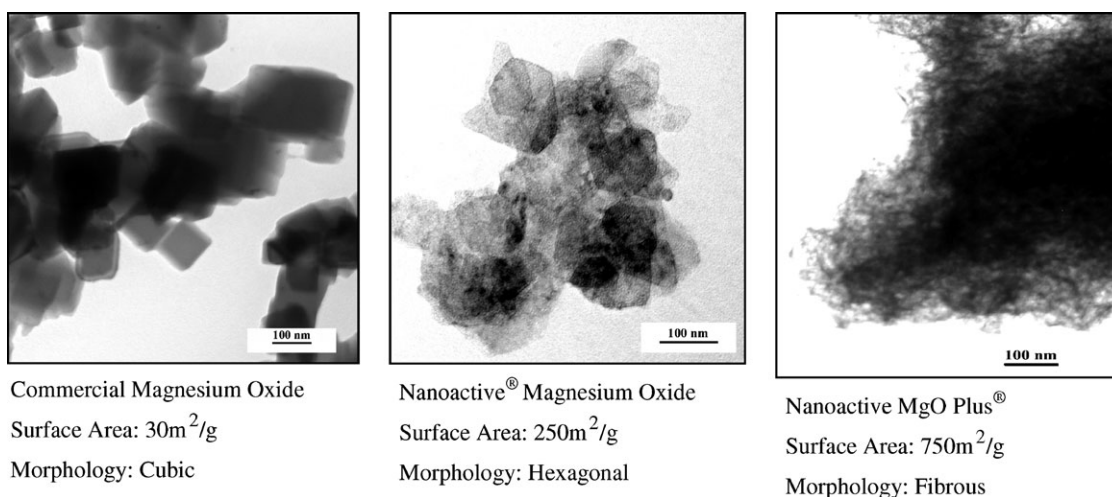


**Fig. 1** Magnesium oxide surface areas and morphologies.

Nanoactive Magnesium Oxide Plus<sup>®</sup> (NA-MgO Plus), all of which are available commercially. In addition, magnesium oxide nanorods are also available *via* laboratory synthesis, but were not a focus of this study.<sup>22</sup>

## 2. Experimental

### 2.1 Materials

A 90% aqueous solution of L(+)-lactic acid from Acros Organics, ACS grade magnesium oxide from Sigma Aldrich (CM-MgO, cubic, 30 m<sup>2</sup> g<sup>-1</sup>) as well as Nanoactive<sup>®</sup> (NA-MgO, hexagonal platelet, 250 m<sup>2</sup> g<sup>-1</sup>) and Nanoactive Plus<sup>®</sup> (NA-MgO Plus, fibrous, 750 m<sup>2</sup> g<sup>-1</sup>) magnesium oxides from NanoScale Corporation were all used without further purification. Fig. 1 summarizes the different shapes and sizes observed in magnesium oxide.

### 2.2 Synthesis of lactic acid–MgO prepolymer

Lactic acid–magnesium oxide composites were synthesized in methanol with 1% by weight loadings of each of the three magnesium oxide materials mentioned above. To begin, the appropriate mass of MgO particles (0.030 g, 0.7 mmol) was suspended in 100 mL of methanol. The mixture was allowed to reflux, with vigorous stirring for 30 min at approximately 65 °C, in order to achieve adequate dispersion of the particles. Approximately 2 g (22 mmol) of lactic acid were added and allowed to react with the suspended particles for 2.5 h. A white precipitate formed upon the addition of lactic acid to each of the three types of MgO. The precipitate formed immediately with commercial MgO and more gradually with the nanoactive samples. Upon completion of the reaction, excess methanol was removed using a rotoevaporator. The product was heat treated at 60 °C (ramp time: 1 h, soak time: 2 h) under vacuum and then left under vacuum overnight in order to remove any trace amounts of solvent from the final product. After drying, the products were collected as semi-solids.

A 5× scale-up synthesis of LA–MgO prepolymer in propanol was achieved by using 10 g (110 mmol) of lactic acid and ~0.15 g (3.7 mmol) of MgO in 150 mL of propanol. The same synthesis and drying procedure as that in methanol

(except reflux temperature went from 65 to 97 °C) was used. After drying, the products were collected as semi-solids.

A prepolymer control was also synthesized using the same procedure as that in propanol. The final LA prepolymer was collected as a clear liquid.

### 2.3 Structural characterization

**2.3.1 NMR analysis.** <sup>1</sup>H and <sup>13</sup>C NMR in *d*<sub>6</sub>-DMSO were obtained for each of the products synthesized in propanol using a Varian Unity 400 MHz NMR.

**2.3.2 FTIR analysis.** Potassium bromide was ground into a fine powder and transparent pellets were prepared using a pellet press. A thin layer of the final products was applied to the pellets and analysis was conducted using a Nexus 670 FTIR spectrophotometer.

### 2.4 Thermal properties

**2.4.1 Melting properties.** Differential scanning calorimetry (DSC) was used to characterize the melting properties, including melting temperature, melting enthalpy, and glass transition temperatures, for each of the aforementioned nanocomposites. A Perkin-Elmer Pyris 1 calorimeter was used in the analysis. The DSC was calibrated with an indium standard and all experiments were performed under a constant flow of nitrogen.

For the sample analysis, approximately 3–4 mg of dried sample were sealed in an aluminium DSC pan for analysis. After holding for 1.0 min at 30 °C, the sample was heated to 170 °C at a rate of 10 °C per minute and then held at this temperature for 3 min in order to eliminate any previous thermal history. The sample was then cooled to –20 °C at –100 °C per minute and held at –100 °C for 3 min. Finally, the sample was heated to 170 °C at 10 °C per minute again. Both the first and second heat scans were recorded. Peak temperatures were used to identify both melting and cold crystallization temperatures and peak areas were to calculate melting enthalpies for each of the samples.

**2.4.2 Thermal stability.** The thermal stability of each of the composites was evaluated using a Shimadzu TGA-50. A constant flow of nitrogen was applied while heating the

samples from 50 to 800 °C at a rate of 10 °C per minute. Commercial MgO, Nanoactive<sup>®</sup>, and Nanoactive MgO Plus<sup>®</sup> were also measured as controls.

## 2.5 Transmission electron microscopy observation

Preparing the samples for TEM analysis involved sonicating each sample in ethanol for 3 min, the result of which was a complete suspension of the product in the solvent. The product was allowed to settle for approximately 30 min and then a drop of the dilute suspension was placed onto a carbon-coated copper grid. Solvent was evaporated from the grid, leaving a thin layer of product on each grid.

TEM analysis was performed using a Philips CM 100 Transmission Electron Microscope (Biology Department, Kansas State University). Liquid nitrogen cooling was necessary to prevent decomposition of the samples under the high vacuum and electron beam environment of the TEM. TEM analysis was conducted on each of the following samples: LA w/CM-MgO, LA w/ NA-MgO, and LA w/NA-MgO Plus, all with 1% loadings of magnesium oxide. Unfortunately, an adequate picture of the prepolymer control was not acquired, as the liquid-like consistency was not conducive to TEM imaging.

## 2.6 Titrimetric analysis of MgO particle consumption by lactic acid

The titrations were carried out by first dispersing 2 g (0.02 mol) lactic acid in 100 mL methanol. 1 g of each of the three types of magnesium oxide was added gradually to the vigorously stirring lactic acid–methanol solution. After each addition, any heat generated was allowed to dissipate. However, addition time intervals were held the same. pH measurements were recorded after each addition and a titration curve was created for each sample.

## 3. Results

### 3.1 Acid–base reactions of different particle morphologies and surface areas

It was important to determine if nanoparticle size and/or the shape differences in the three types of magnesium oxide had an effect on the physical and chemical characteristics of the resulting composite, thus we were very interested in establishing whether or not lactic acid merely consumed the particles upon addition or if the monomer was reacting with the unique surfaces of the different particles. In order to gain this information, titrations were performed assuming that if the particles were being consumed by lactic acid, the equivalence points of each titration would be identical, as surface area and/or shape would not have any effect if this was the case. In contrast, if lactic acid reacts mainly with the surface of the particles (does not progressively etch away and dissolve all of the MgO particles), the surface areas will significantly alter the observed equivalence points.

Titrations were performed by dissolving lactic acid in methanol and then measuring the pH as each of the three MgO materials was added (Fig. 2). A steady increase in the equivalence points was observed as the surface area of the

MgO particles increased indicating that surface area *is* a factor in the reaction between lactic acid and the Nanoactive<sup>®</sup> magnesium oxides.

From the equivalence point masses and the known amount of lactic acid in the sample, it was possible to back-calculate the amount of lactic acid neutralized by each sample of magnesium oxide: CM-MgO: 2.26 mol, NA-MgO: 2.00 mol, NA-MgO Plus: 1.79 mol. These values illustrate that the commercial sample neutralized the most lactic acid with the least amount of MgO, indicating that the primary reaction between lactic acid and CM-MgO was an acid–base

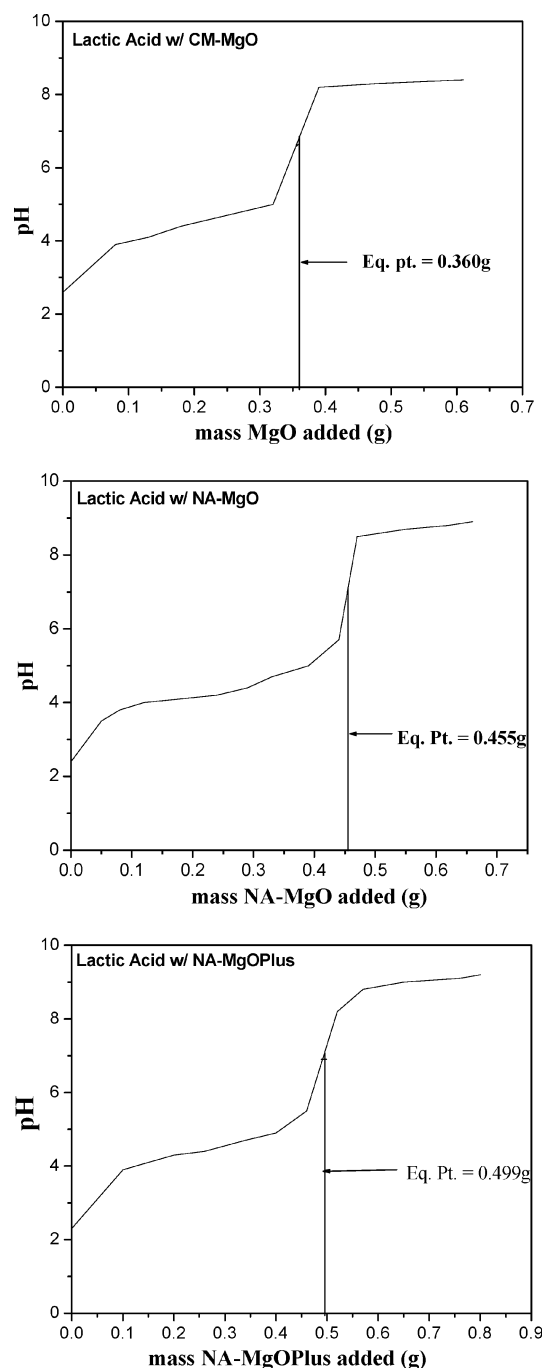


**Fig. 2** Titration curves for lactic acid with CM, NA, and NA-Plus MgO.

neutralization, whereas with the nanoactive samples more metal oxide was required to reach the equivalence point and less lactic acid was neutralized, confirming that while the reaction exhibits some acid–base characteristics, surface reactions were occurring as well. It can be concluded that the larger, less reactive CM-MgO particles reacted more by acid–base neutralization and less by nanoparticle induced polymerization. This is an important observation, and is confirmation that the smaller crystallite, higher surface area materials are more reactive and cause a change in the products of the reaction; that is, more polymerization and less magnesium lactate formation.

### 3.2 Structural characterization *via* infrared analysis

The chemical structure of all specimens was characterized *via* FTIR analysis. The peaks observed, along with their relative intensities, for samples prepared in methanol and propanol are summarized in Table 1 and Table 2, respectively.

The primary peaks were observed for samples prepared in methanol: strong, broad peaks around  $3000\text{ cm}^{-1}$ , attributed to the presence of the hydroxyl functional groups of the lactic acid monomer as well as from water. Sharp, strong peaks around  $1719\text{ cm}^{-1}$  were indicative of a carboxylic acid dimer.<sup>23</sup> Signals at  $1622$  and  $1602\text{ cm}^{-1}$  established that carboxylate ions were a significant product of the reaction. All of the samples showed similar peaks, and it was concluded that the polymerization (ester formation) was only occurring a small amount. Mostly, lactic acid and magnesium lactate were dominant.

Many of the peaks in the samples prepared in propanol are similar to those observed in the samples prepared in methanol. However, the carbonyl asymmetric stretch observed in the methanol solvent system shifted from  $1719\text{ cm}^{-1}$  (mainly carboxylic acid) to  $1735\text{ cm}^{-1}$  signifying an ester linkage.<sup>23</sup> Furthermore, in the presence of CM-MgO, a strong peak at  $1591\text{ cm}^{-1}$  was also observed, which is probably due to the carboxylate anion. This carboxylate peak was very weak or non-existent when NA-MgO or NA-MgO Plus was used. In all cases in refluxing propanol, the strong ester peak was observed at  $1728$  to  $1735\text{ cm}^{-1}$ .

These results indicate that oligomerization/polymerization was facilitated by the higher temperature reaction conditions achieved by refluxing in propanol in place of methanol, as the samples containing Nanoactive<sup>®</sup> MgO showed strong ester signals and no evidence that carboxylate ion was formed as a product of their reaction with lactic acid, whereas in methanol, infrared analysis indicated the presence of carboxylate ion. Interestingly, higher reaction temperatures did not appear to have an effect on the reaction between lactic acid and commercial MgO, as a strong carboxylate peak *was* observed in both the methanol and propanol reaction conditions, which is further confirmation that the size and/or the shape of the

Nanoactive<sup>®</sup> materials influenced the pathway that was taken in the reaction between lactic acid and MgO.

### 3.3 NMR analysis

$^1\text{H}$  and  $^{13}\text{C}$  NMR spectra were obtained for each of the composites. The lactic acid prepolymer, which contained no magnesium oxide, was also analyzed using NMR. The  $^1\text{H}$  NMR spectra were particularly useful in identifying differences between the three composites, in addition to providing evidence that the addition of magnesium oxide, in whatever form, *does* have an effect on the polymerization of lactic acid (Fig. 3 and Fig. 4).

Initially, only minor differences were observed between the four spectra: the triplet located at 3.3 ppm in the prepolymer spectra completely disappeared in the composite samples and the intensities of the peaks vary in each of the four spectra. Closer inspection revealed that these “minor” differences actually confirm that the surface area and/or shape of the MgO additive had a definite effect on the polymerization pathway of lactic acid. Further examination of the spectra was necessary in order to determine exactly *how* polymerization was affected by the addition of magnesium oxide nanoparticles, thus a thorough analysis of each of the spectra follows.

**3.3.1 NMR analysis of lactic acid prepolymer.** In Fig. 3, a very intense multiplet is present at  $\sim 0.86$  ppm, but upon expansion (Fig. 4), a clear doublet (0.87 ppm and 0.82 ppm) of 1 : 2 : 1 triplets emerges. These triplets are likely due to  $-\text{CH}_3$  groups connected to  $-\text{CH}_2$  methyl functionalities, as is common in propyl groups. The fact that there are two separate methyl peaks indicates that there are two similar, but still unique, methyl environments. As these are triplets, it is unlikely that these methyl groups are a part of the polymer, thus they confirm the presence of free propanol and perhaps a propyl ester.

The presence of propanol was expected as it was difficult to completely remove all of the solvent from the product. Further evidence for the presence of free propanol was provided by the multiplet at 1.58 ppm ( $-\text{OCH}_2\text{CH}_2\text{CH}_3$ ) and the triplet at 3.3 ppm ( $-\text{OCH}_2\text{CH}_2\text{CH}_3$ ). The propyl ester, on the other hand, is formed in a likely side reaction, as alcohols and acids commonly react to form ester functionalities. It is our belief that after polymerization of lactic acid is exhausted, propyl ester groups are formed from the reaction of the remaining acid functionalities and free propanol; thus termination of the polymerization reaction is achieved by the formation of propyl ester end groups. Further evidence for these groups shows up at 1.57 ppm ( $-\text{COOCH}_2\text{CH}_2\text{CH}_3$ ) and the triplet at 4.0 ppm ( $-\text{COOCH}_2\text{CH}_2\text{CH}_3$ ).

Evidence for the presence of the polymer is provided by the overlapping peaks between 1.2 and 1.3 ppm. Several overlapping 1 : 1 doublets are present in this section of the

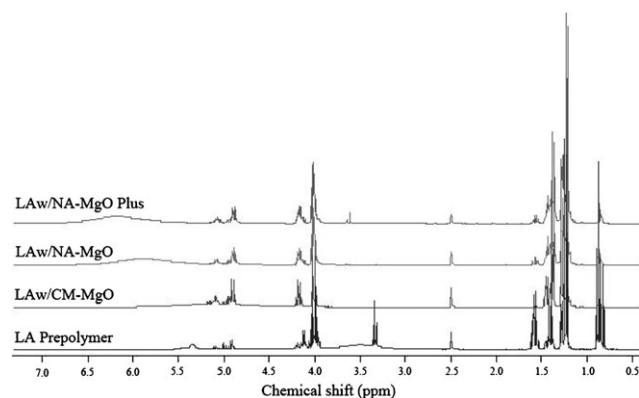
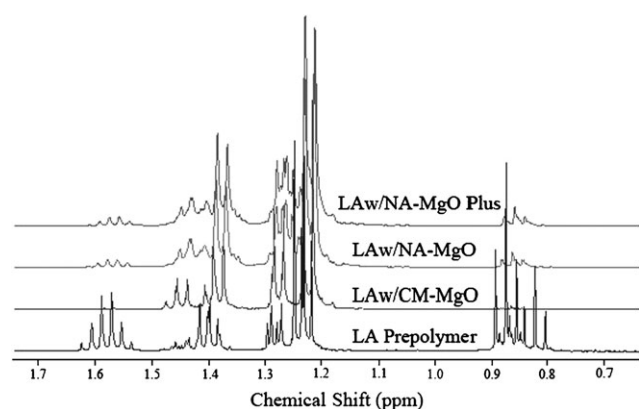
**Table 1** Summary of infrared peaks for LA-MgO composites prepared in MeOH

Sample	Peak frequency/ $\text{cm}^{-1}$
LA:CM-MgO, 1% loading	2984(m, broad), 1719(s), 1626(w), 1454(m), 1373(m), 1205(s), 1123(s)
LA:NA-MgO, 1% loading	2984(m, broad), 1719(s), 1626(w), 1454(m), 1373(m), 1205(s), 1123(s)
LA:NA-MgO Plus, 1% loading	2984(m, broad), 1719(s), 1626(w), 1454(w), 1369(w), 1213(s), 1127(s)



**Table 2** Summary of infrared peaks for LA–MgO composites prepared in propanol

Sample	Peak frequency/cm <sup>-1</sup>
LA prepolymer	3300(m, broad), 1735(s), 1454(m), 1212(m), 1127(s)
LA:CM-MgO, 1% loading	3300(s, broad), 1735(s), 1591(s), 1462(w), 1279(m), 1116(s)
LA:NA-MgO, 1% loading	3300(s, broad), 1731(s), 1475(w), 1373(w), 1209(s), 1123(s)
LA:NA-MgO Plus, 1% loading	3300(s, broad), 1723(s), 1454(w), 1365(w), 1205(m), 1116(s)

**Fig. 3** NMR spectra of lactic acid–MgO composites.**Fig. 4** Expanded NMR spectra (0.7–1.7 ppm) of LA–MgO composites.

spectra, indicating the presence of several similar methyl environments. The doublets indicate that these methyl groups are in close proximity to a –CH group, which is expected as the methyl groups in lactic acid are directly connected to a –CH functionality. The varied chemical shifts of the methyl groups indicate that there were several different polymer environments present in the final product, indicating that perhaps polymerization was stunted by the propanol environment. If this was the case, oligomers could form in many varied sizes, which would change the chemical shifts of the methyl groups slightly. From the expanded spectra (Fig. 4), it appears that there are four overlapping doublets, indicating the presence of four different polymeric methyl groups. A 1 : 2 : 2 : 1 quartet is also present at ~4.0 ppm (overlapping with triplet of propyl ester), which confirms the presence of the methyne proton in the lactic acid polymer. In addition to these peaks, there are also several lower intensity peaks in the spectra at ~4.1 and 5.0 ppm which are probably due to the presence of unreacted lactic acid.

**3.3.2 NMR analysis of LA with CM-MgO.** Upon initial examination of the spectra, it is immediately obvious that very little propanol or propyl ester was present in this sample. The intense peaks between 0.8 and 0.9 ppm are barely visible and the same can be said for the multiplet at 1.58 ppm. Additionally, the multiplet centered at 4.0 ppm in the prepolymer is a clear quartet in this sample, indicating that the methyne proton of lactic acid is still present, but very little if any propyl ester is present. The infrared spectra indicated that carboxylate ion was a primary product of the reaction between lactic acid and commercial MgO, thus it appears that the remaining acid groups were neutralized by the MgO before they could react with propanol to form propyl esters.

As in the prepolymer spectra, several doublet peaks were observed between 1.2 and 1.3 ppm, indicating the presence of varying polymeric methyl environments, thus it appears that some degree of polymerization occurred and as before, it appears that several different sizes were produced in the reaction.

**3.3.3 NMR analysis of LA with NA-MgO and NA-MgO Plus.** The spectra for lactic acid with the Nanoactive<sup>®</sup> and Nanoactive Plus<sup>®</sup> samples are slightly different from that of the sample with commercial MgO. The primary difference is that the aforementioned propyl signals (free propanol and propyl ester), while not as intense as those of the prepolymer, are visible in both spectra, confirming that a decreased number of terminating propyl ester functionalities was formed in the products. The decreased number of terminating groups seems to indicate that polymerization was catalyzed more effectively by the addition of the Nanoactive<sup>®</sup> and Nanoactive Plus<sup>®</sup> MgO particles and as a result, longer chain oligomers were formed.

As in the previous samples, several different polymeric methyl environments were identified, but in these cases, the observed doublets exhibited more complicated structure, which shows that the resulting products were very different than the products discussed previously, as clear doublets were observed in both of the previous cases. Perhaps this is a sign that polymerization has occurred on the surface of the particles. After all, if polymerization *did* occur on the surface of the MgO, the methyl environments would be changed as they would be in close proximity to other polymer chains on the surface of the nanomaterials. It is difficult to say exactly how each of these samples differs, but it is obvious that the addition of magnesium oxide, whether in the commercial form or in the nanosized form, has a direct effect on the polymerization of lactic acid.

By comparison of the peak integrals of the methyl groups within the polymer (1.2 to 1.3 ppm) with the propyl ester at 1.58 for the NA-MgO Plus, the ratio of the number of methyl

groups within the polymer to propyl ester terminal groups is about 15. This would suggest that low molecular weight polymers of about 15 repeating units were formed.

Furthermore, there are differences between the NA-MgO, NA-MgO Plus and the CM-MgO. With the latter oxide, very little propyl ester was formed, and this may be due to the fact that CM-MgO favors acid–base chemistry with lactic acid, while the Nanoactive<sup>®</sup> samples favor polymerization chemistry.

### 3.4 TEM analysis of composites

Infrared and NMR analyses were very useful as both methods provided a means of confirming which functional groups were present in the products and identifying any obvious differences in the chemical environments of the three composites. However, more information regarding the nature of the reaction as well as the physical changes that occurred by adding MgO to the lactic acid matrix were necessary in order to gain insight into how surface area and shape really affect the polymerization of lactic acid. Therefore, the composites were also examined under a TEM in order to get a better idea of how the chemical differences were manifested on a physical level.

With CM-MgO in refluxing propanol, very little polymerization took place, as only short remnants of polymer material were observed (Fig. 5). Therefore, it can be deduced that while the primary reaction between lactic acid and commercial MgO is an acid–base neutralization reaction, at propanol reflux temperatures, polymerization is enhanced. In this case, polymerization was initiated at numerous sites due to the higher reaction temperature, which results in the vast number of polymer units observed under the microscope.

Nanoactive<sup>®</sup> MgO performed very well in methanol, as long-chain, interconnected polymer strands were observed (Fig. 6A), indicating that the presence of the nanomaterial catalyzed polymerization of the monomer. At higher temperatures in propanol, the effect of adding NA-MgO was even greater. Long-chain, highly interconnected and crosslinked materials can be seen in Fig. 6B, indicating that polymerization was further induced by the higher reaction temperature. Additionally, by comparing Fig. 5 with Fig. 6, it is easy to see that the products physically are very unique and this uniqueness *must* be due to the differences in surface area and/or shape of the magnesium oxide additive. If our hypothesis is correct, initiation of polymerization occurs at the surface of the particles, which would produce several strands on the surface of a particle, which could then interconnect and crosslink, much like that which is observed in the TEM image.

With the highest surface area and most reactive NA-MgO Plus, in propanol, star-shaped materials (Fig. 7A) were observed, whereas in methanol, flower-like materials (Fig. 7B) were the norm. These collections of oligomer strands have voids in the center and as a result, it is difficult to analyze exactly how lactic acid reacts with the surface of these materials, as NA-MgO Plus is a fibrous material. It is possible that during reflux, the nanoparticles interact with each other to form a circular structure, which the lactic acid then reacts with. In this case, polymerization still initiates on the surface of the

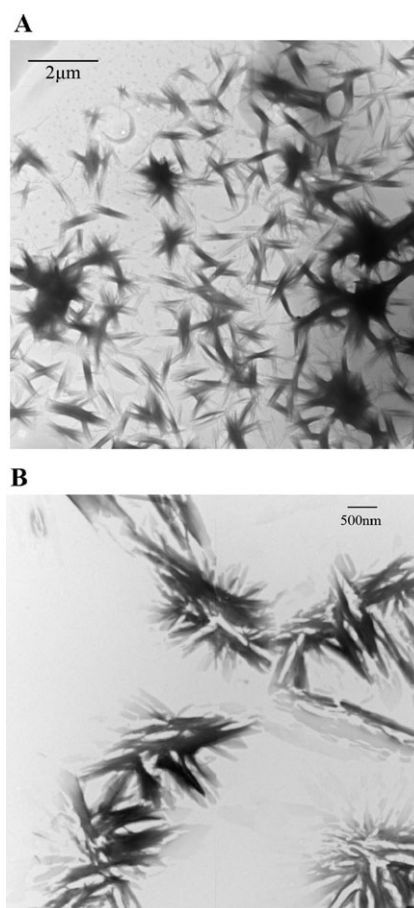


**Fig. 5** TEM images of LA w/CM-MgO (1% loadings) prepared in (A) propanol, and (B) methanol.

material and then continues until termination occurs. Again, it is obvious that surface reactions were occurring and they absolutely have an effect on the physical characteristics of the resulting polymer.

### 3.5 Thermal properties

All of the lactic acid–magnesium oxide composites showed melting temperatures in the first heat-scanning (Fig. 8). The prepolymer composite with NA-MgO Plus had the sharpest melting peak while the composite with CM-MgO presented two broad melting peaks. In between the two extremes, the composite containing NA-MgO produced a single, slightly broadened melting peak. The second heating scan produced very different results. Fig. 8 shows that a melting peak, while slightly lower than in the first heating scan, was observed for the NA-MgO Plus composite, while no melting temperatures could be derived for the remaining composites. The sharpness of the melting peaks also suggests that the arrangements of polymer chains formed in the prepolymers with NA-MgO Plus and NA-MgO were more uniform in nature than that of the composites with CM-MgO.

Perhaps the most interesting data, however, are the actual melting temperatures, summarized in Table 3. The highest melting point was observed in the prepolymer composite with NA-MgO Plus, which suggests that the star-shaped structures

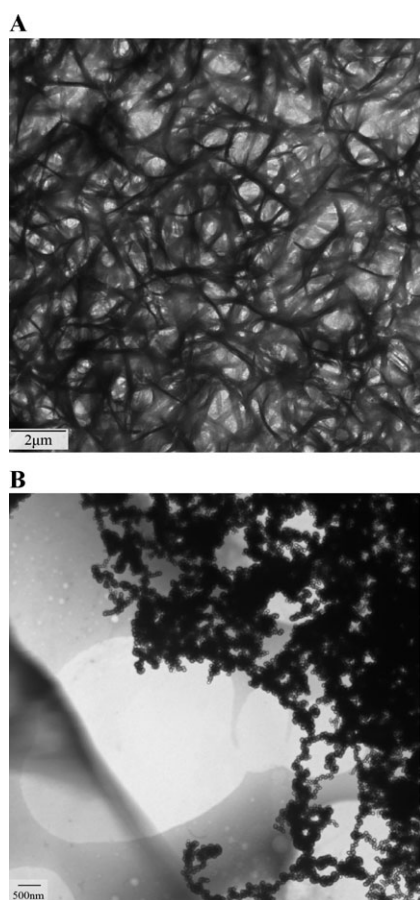


**Fig. 6** TEM images of LA w/NA-MgO (1% loadings) prepared in (A) propanol, and (B) methanol.

observed in the TEM are more uniform and thermally stable than the other two composites. In addition, the composite containing NA-MgO Plus showed the largest melting enthalpy, while the prepolymer with CM-MgO had the smallest melting enthalpy.

TGA analysis of the three composites strongly suggests that more thermally stable materials were formed when nanoparticles of magnesium oxide were allowed to interact with lactic acid. Note from Fig. 9 that the LA-prepolymer decomposed at rather low temperatures, and by 350 °C essentially 100% weight loss had occurred. However, in the case of the MgO-LA composites, much higher temperatures were required to cause decomposition and weight loss. Thus, in the range of 200–350 °C, the polymer composites lost about 40–60% of their mass, and between 350 and 500 °C, about 90%.

#### 4. Discussion

Several papers have been published regarding the use of nanoclays in petroleum-based polymers and plastics,<sup>13–16</sup> but the use of metal oxide reactive nanoparticles in biopolymers is very new.

Our research focused on the use of magnesium oxide as both a reactant and polymerization template for lactic acid. Of particular interest was the chemistry that occurred between the

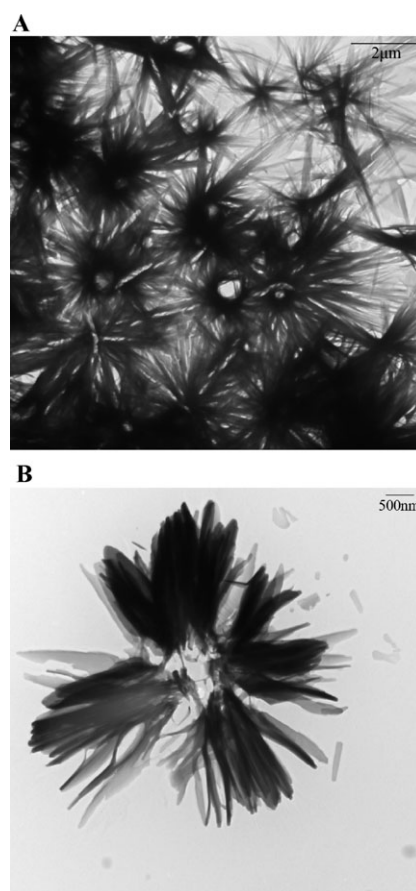


**Fig. 7** TEM images of LA w/NA-MgO Plus (1% loadings).

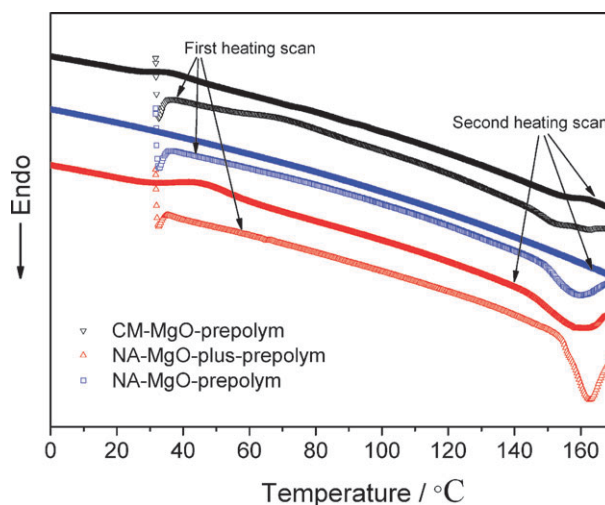


**Fig. 8** DSC curves for lactic acid-MgO composites.

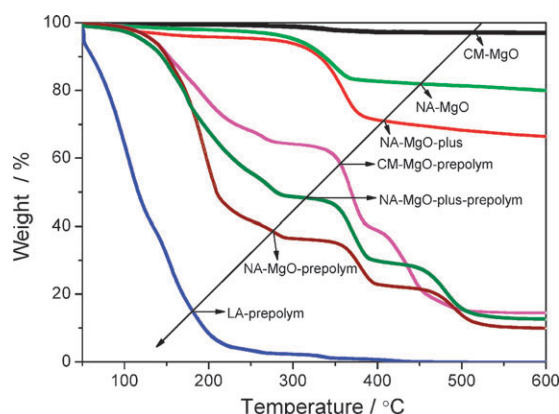
two. NMR, FTIR, UV-Vis, and TEM were all used to characterize the chemical differences resulting from the addition of Commercial MgO, Nanoactive<sup>®</sup>, or Nanoactive Plus<sup>®</sup> magnesium oxide.

Titration of lactic acid were performed with each of the three types of MgO in addition to the testing listed above. The results of the titrations indicated that the surface area and reactivity of the different materials had an effect on the



**Table 3** DSC analysis of lactic acid–MgO composites

Sample		$T_m/^\circ\text{C}$	$\Delta H_m/\text{J g}^{-1}$
LA w/CM-MgO	First heating scan	151	14
	Second heating scan	162	8.4
LA w/NA-MgO	First heating scan	159	31
	Second heating scan	—	—
LA w/NA-MgO Plus	First heating scan	163	40
	Second heating scan	158	31

**Fig. 9** TGA of lactic acid–MgO composites and pure MgO samples.

reaction pathway. For example, commercial MgO neutralized the most lactic acid with the least amount of material indicating that the primary reaction between lactic acid and commercial MgO is a neutralization reaction. In contrast, more material was required to reach an equivalence point with the nanoactive samples, confirming that while a neutralization reaction still occurs, there are also competing surface reactions between the lactic acid and the surface –OH groups. These surface reactions appear to be the points of initiation for polymerization of lactic acid on the surface of the MgO nanoparticles.

With this in mind, NMR and IR analyses were performed on each of the different composites in order to confirm these results. At high temperatures, a strong carboxylate peak in the sample containing commercial MgO was obvious, but very little evidence of carboxylates was observed in the composites with the nanoactive MgO samples, confirming that an acid–base reaction was not the primary pathway in the reaction between lactic acid and the more reactive MgO nanoparticles. Additionally, NMR analysis showed very complex methyl environments in the nanocomposites, indicating that substantially different materials were produced with each material.

TEM provided perhaps the most interesting piece of the puzzle. The images indicate that not only does the surface area and reactivity of the additive affect the chemical properties of the resulting composites, but also the physical properties. The images show that the composites with nanoparticles produced materials with high polymer content, as expected from the previous results. However, the initiation of polymerization appears to be different with each material, as long, interconnected strands were observed in the composites containing NA-MgO, and circular, star-shaped materials were observed

with NA-MgO Plus. This indicates that in addition to surface area, the *shape* of the nanoparticles also affects the resulting physical and chemical properties of the composites. However, it should be added that a clear understanding of the chemical details regarding initiation and propagation is lacking, but special reactive sites or “hot spots” on the nanoparticle surface seem to be important, and this is why *shape* matters. Indeed, these reactive sites could be due to a combination of site geometry and thermal effects due to exothermicity of reactions at that site.

Thermal stability was also an important part of this study, as one of the issues with the use of lactic acid is its stability when heated above its glass transition temperature. TGA and DSC analyses were performed in order to examine how the addition of nanoparticles affects this stability. The results indicate that more thermally stable materials, with decomposition temperatures above 350 °C, were produced in this study.

The future of this project lies primarily in furthering the polymerization of the prepolymer nanocomposites made in this study to form full PLA composites. The chemical, physical, thermal, and rheological properties of the full polymers could then be compared with that of commercial PLA. Additionally, other metal oxide nanoparticles, such as calcium oxide, zinc oxide, or titanium oxide, have potential as additives to biopolymers. This work is still in its infancy, but has definite potential to both change and improve the nature and use of bioplastics.

## Acknowledgements

The support of the Kansas State University Center for Biopolymers by Design and the Women in Science Program (Advance) is acknowledged with gratitude. We especially thank Professor Duy Hua for helpful discussions.

## References

- 1 A. Kaleel and R. M. Richards, in *Nanoscale Materials in Chemistry*, ed. K. J. Klabunde, Wiley Interscience, New York, NY, 2001, ch. 4, pp. 85, 223.
- 2 K. J. Klabunde, J. V. Stark, O. Koper, C. Mohs, D. G. Park, S. Decker, Y. Jiang, I. Lagadic and D. Zhang, *J. Phys. Chem.*, 1996, **100**, 12142–12153.
- 3 S. C. Emerson, C. F. Coote, H. Boote, J. C. Tufts, R. LaRocque and W. K. Moser, *Surf. Sci. Catal.*, 1998, **118**, 773.
- 4 B. M. Choudary, R. S. Mulukutla and K. J. Klabunde, *J. Am. Chem. Soc.*, 2003, **125**, 2020–2021.
- 5 M. L. Kantam, S. Laha, J. Yadov and B. Sreedhar, *Tetrahedron Lett.*, 2006, **47**, 6213.
- 6 M. L. Kantam, R. B. Chakrapani and B. M. Choudary, *Tetrahedron Lett.*, 2007, **48**, 6121.
- 7 F. G. Gault, *Adv. Catal.*, 1981, **30**, 1.
- 8 C. Corrolleur, F. G. Gault, D. Juttard, G. Maire and J. M. Muller, *J. Catal.*, 1972, **27**, 466.
- 9 C. Corrolleur, S. Corrolleur and F. G. Gault, *J. Catal.*, 1972, **24**, 385.
- 10 G. Vitulli, E. Pitzalis, A. Verazzani, P. Alessandra, P. Pertici, P. Slavador and G. Martra, Part 2, *Synthesis and Properties of Mechanically Alloyed and Nanocrystalline Materials*, *Mater. Sci. Forum*, 1997, 235.
- 11 M. Boudart, A. W. Aldag, J. E. Benson, N. A. Dougharty and G. G. Harkins, *J. Catal.*, 1966, **6**, 92.
- 12 S. C. Davis and K. J. Klabunde, *Chem. Rev.*, 1982, **82**, 153.



- 13 R. P. Wool and X. S. Sun, *Bio-Based Polymers and Composites*, Elsevier, New York, NY, 2005.
- 14 Z. S. Petrovic, I. Javni, A. Waddon and G. Banhegyi, *J. Appl. Polym. Sci.*, 2000, **76**, 133–151, and references therein.
- 15 R. M. Johnson, L. Y. Mwaikambo and N. Tucker, *Biopolymers*, 2003, **14**, 1–26.
- 16 Y. B. Vasudeo and M. Bausmina, *Prog. Mater. Sci.*, 2005, **50**, 962–1079.
- 17 M. Avella, M. E. Errico and G. Gentile, *Macromol. Symp.*, 2007, **247**, 140–146.
- 18 (a) B. Wang, X. S. Sun and K. J. Klabunde, *J. Biobased Mater. Bioenerg.*, in press; (b) At the full polymer stage, a low loading of 1% by weight or less of MgO nanomaterials imparts beneficial properties, whereas higher loadings generally led to more brittleness and loss of transparency. For this reason, most of the work herein on the prepolymer was done with 1% by weight loadings.
- 19 M. P. Pelini, *J. Phys. Chem. C*, 2007, **111**, 9019–9038.
- 20 M. Brust, M. Walker, D. Bethell, D. Schiffrin and R. Whymann, *J. Chem. Soc., Chem. Commun.*, 1994, 801–802.
- 21 J. A. Dahl, L. S. Maddux and J. E. Hutchison, *Chem. Rev.*, 2007, **107**, 2228–2269.
- 22 P. Jeevanandam, R. S. Mulukutla, Z. Yang, H. Kwen and K. J. Klabunde, *Chem. Mater.*, 2007, **19**, 5395–5403.
- 23 R. M. Silverstein, F. H. Webster and D. J. Kiemie, *Spectroscopic Identification of Organic Compounds*, John Wiley and Sons, New York, 2005, pp. 100, 102–103.